

Spin-orbit coupling and ESR theory for carbon nanotubes

A. De Martino,¹ R. Egger,¹ K. Hallberg,² and C.A. Balseiro²

¹ *Institut für Theoretische Physik, Heinrich-Heine Universität, D-40225 Düsseldorf, Germany*

² *Instituto Balseiro, Centro Atómico, 8400 S.C. de Bariloche, Argentina*

(Date: May 21, 2019)

A theoretical description of ESR in 1D interacting metals is given, with primary emphasis on carbon nanotubes. The spin-orbit coupling is derived, and the resulting ESR spectrum is analyzed by field theory and exact diagonalization. Drastic differences in the ESR spectra of single-wall and multi-wall nanotubes are found. For single-wall tubes, the predicted double peak spectrum could reveal spin-charge separation.

PACS numbers: 71.10.-w, 73.63.Fg, 76.30.-v

Electron spin resonance (ESR) serves as a valuable tool to experimentally probe the intrinsic spin dynamics of many systems. In ESR experiments one applies a static magnetic field and measures the absorption of radiation polarized perpendicular to the field direction. In the absence of $SU(2)$ spin symmetry breaking terms in the system Hamiltonian, the absorption intensity is then simply a δ -peak at the Zeeman energy [1]. Since spin-orbit (SO) interactions are generally the leading terms breaking the $SU(2)$ invariance, deviations in the ESR intensity from the δ -peak, e.g. shifts or broadenings, are directly connected to these couplings. In this Letter we theoretically address the spin-orbit interaction and the resulting ESR spectrum for interacting 1D metallic conductors, in particular for carbon nanotubes. Nanotubes constitute a new class of mesoscopic quantum wires characterized by the interplay of strong electron-electron interactions, reduced dimensionality, disorder, and unconventional spin dynamics [2–6]. ESR is an important technique to elucidate aspects of this interplay inaccessible to (charge) transport experiments. For interacting many-body systems, surprisingly little is known about ESR although it represents an interesting theoretical problem.

Two main classes of nanotubes may be distinguished, namely single-wall nanotubes (SWNTs) which consist of just one wrapped-up graphite sheet, and multi-wall nanotubes (MWNTs). MWNTs contain additional inner shells, but transport is generally limited to the outermost shell [4]. Evidence for the Luttinger liquid (LL) behavior of interacting 1D electrons has been reported for charge transport in SWNTs [3], where one also expects to find spin-charge separation [5,6]. Conventional wisdom holds that the SO coupling in 1D conductors always destroys spin-charge separation [7]. Below we show that this statement is *incorrect*. In fact, the SO interaction considered in Ref. [7] only applies to the limited class of semiconductor quantum wires in strong Rashba

and confinement electric fields, but does not represent the generic SO Hamiltonian for other 1D conductors. The latter is derived below and determines the ESR intensity in SWNTs and MWNTs. A totally different ESR spectrum compared to semiconductor wires emerges. In particular, the single δ -peak is split into *two* narrow peaks in SWNTs, while in semiconductor wires the spectrum forms a broad band with thresholds at the lower and upper edge [8]. This qualitative difference can be traced back to the fact that the SO interaction in SWNTs [see Eq. (5) below] does *not* spoil spin-charge separation. Experimental observation of the peak splitting could therefore provide direct evidence for the elusive phenomenon of spin-charge separation. In MWNTs, inner shells cause a rather strong Rashba-type SO coupling, leading instead to a *single* narrow ESR peak. To experimentally observe our predictions, it will be crucial to work with samples free of magnetic impurities whose presence has drastically affected previous ESR measurements for nanotubes [4].

In the standard Faraday configuration, the ESR intensity at frequency ω is proportional to the Fourier transform of the transverse spin-spin correlation function [1],

$$I(\omega) = \int dt e^{i\omega t} \langle S^+(t) S^-(0) \rangle, \quad (1)$$

where the static magnetic field points along the z -axis and $\vec{S} = \sum_i \vec{S}_i$ is the total spin operator. Equation (1) is connected to the dynamical susceptibility via $I(\omega) \sim \omega \chi''(\omega)$. The Hamiltonian is $H = H_0 + H_Z + H'$, where H_0 represents the $SU(2)$ invariant nanotube Hamiltonian including electron-electron interactions, $H_Z = -BS^z$ is the Zeeman term [9], and H' represents $SU(2)$ breaking terms, in particular the SO coupling. Inserting a complete set of eigenstates $|a\rangle$ of H in Eq. (1), the ESR intensity follows as

$$I(\omega) = \frac{1}{Z} \sum_{a,b} e^{-E_b/T} \delta(\omega - (E_a - E_b)) |\langle a | S^- | b \rangle|^2.$$

If H is $SU(2)$ invariant (apart from H_Z), $I(\omega)$ only receives contributions from matrix elements between eigenstates with equal total spin $S_a = S_b$. Then all states with $S_a^z = S_b^z - 1$ will contribute to form a δ -peak at frequency $\omega = B$. At zero temperature, the application of a magnetic field B , taken as large enough to overcome a spin gap possibly present at $B = 0$, leads to a ground state with finite magnetization, $S_0 \neq 0$, and the states with

$S_a^z = S_0^z - 1$ yield the δ -peak. Any perturbation preserving $SU(2)$ invariance will neither shift nor broaden this peak, even at finite temperature, and it is therefore crucial to identify H' . For quantum spin chains, staggered magnetic fields and Dzyaloshinskii-Moriya interactions have been emphasized [1].

Let us start with the derivation of the SO interaction in nanotubes. In this derivation we neglect electron-electron interactions which only weakly renormalize the SO strength [10]. In a single-particle picture, the SO interaction then appears because an electron moving in the electrostatic potential $\Phi(\vec{r})$, e.g. due to the ions, sees an effective magnetic field $\vec{v} \times \nabla\Phi$. With $\vec{p} = m\vec{v}$ and the standard Pauli matrices $\vec{\sigma}$, the SO interaction reads in second-quantized form:

$$H' = -\frac{ge\mu_B}{4m} \int d\vec{r} \Psi^\dagger [(\vec{p} \times \nabla\Phi) \cdot \vec{\sigma}] \Psi. \quad (2)$$

The electron spinor field $\Psi_\sigma(\vec{r})$, defined on the wrapped graphite sheet, can be expressed in terms of the electron operators c_i for honeycomb lattice site i at \vec{r}_i , $\Psi_\sigma(\vec{r}) = \sum_i \chi(\vec{r} - \vec{r}_i) c_{i\sigma}$, where $\chi(\vec{r})$ is the $2p_z$ orbital wavefunction. The localized orbitals can be chosen as real-valued functions even when hybridization with $2s$ orbitals is taken into account, but their specific form is of no immediate interest here. We then obtain the SO interaction, see also Ref. [11],

$$H' = \sum_{\langle jk \rangle} ic_j^\dagger (\vec{u}_{jk} \cdot \vec{\sigma}) c_k + \text{h.c.} \quad (3)$$

which indeed breaks $SU(2)$ symmetry. With obvious modifications, Eq. (3) applies to other 1D conductors and thus represents a generic SO Hamiltonian. The SO vector $\vec{u}_{jk} = -\vec{u}_{kj}$ has real-valued entries,

$$\vec{u}_{jk} = \frac{ge\mu_B}{4m} \int d\vec{r} \Phi(\vec{r}) [\nabla\chi(\vec{r} - \vec{r}_j) \times \nabla\chi(\vec{r} - \vec{r}_k)]. \quad (4)$$

The on-site term ($j = k$) is identically zero, and since the overlap decreases exponentially with $|\vec{r}_j - \vec{r}_k|$, we keep only nearest-neighbor terms in Eq. (3).

Let us first turn to SWNTs, where SO couplings are expected to be small. This can be rationalized from our approach since the SO vector (4) *vanishes* by symmetry for an ideal 2D honeycomb lattice. A finite (nearest-neighbor) SO coupling can only arise due to the curvature of the wrapped sheet, stray fields from nearby gates, or due to defects, all of which break the high symmetry and in principle allow for significant SO couplings [6]. Focusing on the curvature-induced SO coupling, the SO vector only depends on bond direction, $\vec{u}_{\vec{r}_i, \vec{r}_i + \vec{\delta}_a} = \vec{u}_a$, for the nearest-neighbor bonds $\vec{\delta}_a$ ($a = 1, 2, 3$) of the graphite sheet [2]. To make progress, we employ the effective field theory approach [5]. Neglecting the (here inessential) ‘‘flavor’’ index due to the presence of two K points

[2], H_0 then corresponds to a spin-1/2 LL described by charge/spin interaction parameters $K_c < 1$, K_s and velocities $v_{c/s} = v_F/K_{c/s}$ with the Fermi velocity $v_F = 8 \times 10^5$ m/sec; $SU(2)$ invariance of H_0 fixes $K_s = 1$ [12]. The LL Hamiltonian completely decouples when expressed in terms of spin and charge boson fields [12], and the Zeeman term H_Z only affects the spin sector. Written in terms of right- and left-moving fermions $\psi_{R/L}$, the continuum version of Eq. (3) is (up to irrelevant terms) $H' = H_1 + H_2$ with

$$H_1 = \int dx \vec{\lambda} \cdot (\vec{J}_L - \vec{J}_R), \quad (5)$$

$$H_2 = \int dx \sum_{r=R/L} \psi_r^\dagger \vec{\lambda}' \cdot \vec{\sigma} i\partial_x \psi_r + \text{h.c.} \quad (6)$$

With the unit vector \hat{e}_t along the tube axis, we use

$$\vec{\lambda} = 2 \text{Im} \sum_a e^{i\vec{K} \cdot \vec{\delta}_a} \vec{u}_a, \quad \vec{\lambda}' = \sum_a e^{i\vec{K} \cdot \vec{\delta}_a} (\hat{e}_t \cdot \vec{\delta}_a) \vec{u}_a,$$

and neglect oscillatory terms which average out on large length scales. These oscillations are governed by the wavevector $2k_F$ corresponding to the doping level μ , $k_F = |\mu|/v_F$, with typical values $|\mu| \approx 0.3$ to 0.5 eV [13]. Finally, $\vec{J}_{R,L} = \psi_{R/L}^\dagger (\vec{\sigma}/2) \psi_{R/L}$ are the standard $SU(2)$ spin currents. The perturbation (5) has scaling dimension 1 (relevant) whereas Eq. (6) has dimension 2 (marginal). Therefore the leading SO contribution retained in what follows is Eq. (5).

Remarkably, the SO interaction then acts exclusively in the spin sector and hence does *not spoil spin-charge separation*. As a consequence, since electron-electron interactions affect only the charge sector, the ESR intensity can be computed using the equivalent fermionic spin Hamiltonian

$$H_f = \sum_{r=R/L=\pm} \int dx \left[-irv_s \psi_r^\dagger \partial_x \psi_r + \vec{\lambda}_r \cdot \vec{J}_r \right], \quad (7)$$

where $\vec{\lambda}_\pm = \vec{B} \pm \vec{\lambda}$. Since H_f is bilinear in the fermions, the exact ESR spectrum follows for arbitrary temperature,

$$I(\omega) = \sum_{r=\pm} \left(1 + \frac{\lambda_r^z}{\lambda_r} \right)^2 \frac{\lambda_r}{4v_s(1 - e^{-\lambda_r/T})} \delta(\omega - \lambda_r), \quad (8)$$

with $\lambda_\pm = |\vec{\lambda}_\pm|$. As a consequence of SO coupling, the single δ -peak *splits into two peaks* but there is no broadening. The peak separation is $|\lambda_+ - \lambda_-|$, and the peak heights are generally different. To lowest order in λ/B , the two peaks are located symmetrically around $\omega = B$. Notice that for \vec{B} perpendicular to the effective SO vector $\vec{\lambda}$, the splitting is zero. It should be stressed that these results hold both for the non-interacting and the interacting case. In the latter case, they crucially rely on

spin-charge separation since otherwise the charge sector will mix in, leading to broad bands with threshold behaviors [8]. We mention in passing that inclusion of a small $\vec{\lambda}'$ preserves the splitting into two peaks, but the peaks now acquire a finite width $\sim |\vec{\lambda}'|$.

In practice, to get measurable intensities, one has to work with an ensemble of SWNTs. In many cases, unless one works with ordered arrays, the SO vector $\vec{\lambda}$ can then take any direction. Assuming a uniform probability distribution for the orientation of $\vec{\lambda}$, the average can easily be done. For $T = 0$ and $\vec{\lambda}' = 0$, we find

$$\overline{I(\omega)} = \frac{[(\omega + B)^2 - \lambda^2]^2}{16v_s B^3 \lambda} \theta(B + \lambda - \omega) \theta(\omega - |B - \lambda|) \quad (9)$$

with the Heaviside function $\theta(z)$. For $B > \lambda$, this asymmetric spectrum has the width $\Delta\omega = 2\lambda$, which in turn allows to extract the SO coupling strength from ESR measurements.

To put these results into a broader perspective and to make contact to other 1D conductors, it is useful to consider the familiar 1D Hubbard chain [12] with uniform SO coupling,

$$H = \sum_{\langle ij \rangle} c_i^\dagger \left(-t + i\vec{\lambda} \cdot \vec{\sigma} \right) c_j + \text{h.c.} \quad (10)$$

$$+ U \sum_i n_{i\uparrow} n_{i\downarrow} - B \sum_i S_i^z.$$

For $\vec{\lambda} = 0$, Eq. (10) leads to a LL phase at low energies [12]. The generalization of Eq. (10) to a two-leg Hubbard ladder directly describes SWNTs with short-range Coulomb interactions [14]. We have calculated the ESR spectrum using exact diagonalization for small lattices. While Eq. (8) directly applies to SWNTs, the Hubbard chain is of more relevance to other 1D conductors, e.g. chain molecules, where strong effects of band curvature and discrete translational invariance are expected. In addition, the exact solution of Eq. (10) without SO interaction [12] shows that magnetic fields mix charge and spin sectors, which could also modify Eq. (8).

The main features emerging from exact diagonalization can be seen in Fig. 1. For weak interactions, see Fig. 1(a), we recover the two-peak structure (8), with the peaks symmetrically arranged around $\omega = B$ but with different peak heights. In addition, no splitting is seen for \vec{B} perpendicular to the SO vector $\vec{\lambda}$. The interaction dependence of the ESR spectrum is shown in Fig. 1(b). Strong interactions suppress one of the peaks and enhance the other, and also give rise to more structure in the spectrum. This behavior can be traced back to the effects of band curvature. Note that for increasing U , the distance between both peaks decreases. This behavior can be quantitatively explained by a decrease of the spin velocity v_s with U [15].

For the remainder, we focus on MWNTs where we first contemplate a simple two-shell model. Experimental evidence [4] is consistent with the assumption that inter-shell tunneling is strongly suppressed. Therefore doping due to charge transfer from the substrate, the attached leads, or due to oxygen absorption, should only affect the outermost shell, while $\mu \approx 0$ for inner shells. Under this assumption, basically all conduction electrons contributing to the ESR signal reside in the outermost shell. Moreover, the electrostatic potential Φ_o of the outer shell differs from the inner-shell potential Φ_i . In effect, we can then restrict attention to the outermost shell (of radius R) alone, but in a radial electric field of size $E \approx 2c_{12}\Delta\Phi/R$, where c_{12} is the inter-shell capacitance per length and $\Delta\Phi = \Phi_i - \Phi_o$. The general expression (4) for the SO vector then yields after some algebra for a given bond $\vec{\delta}_a$

$$\vec{u}_a = (u/v_F) \hat{E} \times \vec{\delta}_a, \quad (11)$$

where \hat{E} is a unit vector perpendicular to the tube surface, and $u \approx c_{12}e\Delta\Phi/(m^2dR)$ with the C-C distance $d = 1.42 \text{ \AA}$. To proceed, we turn to the low-energy theory, again for only one K point. The influence of interactions is expected to be less dramatic in MWNTs compared to SWNTs, and here we focus on the non-interacting case. In real space, we then have a Dirac Hamiltonian, $H_0 = -iv_F \int d\vec{r} \Psi^\dagger (\vec{\tau} \cdot \vec{\nabla}) \Psi$, where the integral extends over the tube surface and the Pauli matrices $\vec{\tau}$ act in sublattice space. The SO contribution appropriate for MWNTs follows by inserting Eq. (11) into Eq. (3), which yields the manifestly Hermitian term

$$H' = -iuv_F \int d\vec{r} \Psi^\dagger (\tau^- \sigma^+ - \tau^+ \sigma^-) \Psi. \quad (12)$$

We take the magnetic field parallel to the tube axis and include both orbital and Zeeman contributions [16]. The full Hamiltonian can then be diagonalized. The dispersion relation contains four branches, $\epsilon_\pm(\vec{k}) = \pm\epsilon_\pm(k)$, where the \pm signs are independent and

$$\epsilon_\pm(k) = \left[v_F^2(k^2 + Q^2) + (B/2)^2 \pm v_F \right. \quad (13)$$

$$\left. \times \left\{ (B^2 + 2v_F^2 Q^2)k^2 + v_F^2 Q^4 \right\}^{1/2} \right]^{1/2},$$

with $Q = 2\sqrt{2}u$ measuring the SO strength and $k = |\vec{k}|$. Using Eq. (13), the ESR intensity reads

$$I(\omega) = \int_\Omega d\vec{k} \frac{\pi}{2\epsilon_+ \epsilon_-} \frac{\Pi(\epsilon_+, k; \omega)}{(\epsilon_+^2 - \epsilon_-^2)^2} \delta(\omega - \epsilon_+ + \epsilon_-), \quad (14)$$

where the integration region Ω in \vec{k} -space is defined by

$$\epsilon_-(k) \leq \mu \leq \epsilon_+(k). \quad (15)$$

This $T = 0$ result is readily generalized to finite temperatures [15]. The integral in Eq. (14) includes an integration over the momentum parallel to the MWNT axis and

a discrete summation over the quantized transverse momenta, $k_{\perp} = (n - \phi)/R$, where $\phi = \pi R^2 B/(h/e)$ is due to the orbital effect of the applied magnetic field and the summation extends over integer n . Furthermore, with $\bar{\omega}' = \omega' - \omega$ and $f(\omega', k) = v_F^2 k^2 - (B/2 + \omega')^2$,

$$\begin{aligned} \Pi(\omega', k; \omega) = & 2f(\omega', k)f(-\bar{\omega}', k) \times \\ & [(B/2 - \omega')(B/2 + \bar{\omega}') - v_F^2 k^2] \\ & - 2v_F^2 Q^2 [(B/2 - \omega')(B/2 - \bar{\omega}')f(\omega', k) \\ & + (B/2 + \omega')(B/2 + \bar{\omega}')f(-\bar{\omega}', k)]. \end{aligned} \quad (16)$$

As a simple check, for $Q = 0$ one recovers the expected δ -peak from Eq. (14).

The result (14) can be understood in simple physical terms. The ESR intensity receives contributions from transitions between states of energy ϵ_- to states of energy ϵ_+ , so long as the ϵ_- (ϵ_+) state is occupied (empty), which is precisely ensured by the condition (15). In order to arrive at Eq. (14), we have neglected a contribution coming from transitions between $-\epsilon_{\pm}$ and ϵ_{\mp} states. This is consistent because these transitions only contribute for very large frequencies $\omega \geq |\mu|$, while the frequency scales $\omega \approx B$ relevant to ESR are much lower. Inspection of Eq. (14) shows that the ESR spectrum of a MWNT contains only a *single narrow peak* centered at $\omega = (B^2 + 2v_F^2 Q^2)^{1/2}$, with linewidth $\Delta\omega \approx v_F^2 Q^2 B^2 / \mu^3$. (For the detailed lineshape and its temperature dependence, see Ref. [15].) The ESR spectra of SWNTs and MWNTs are therefore fundamentally different and reflect distinct mechanisms of spin-orbit coupling.

To conclude, we have presented a theoretical description of the spin-orbit coupling and the ESR spectrum for 1D conductors, in particular for carbon nanotubes. In SWNTs, spin-charge separation should not be affected by spin-orbit coupling, and hence we expect a double peak. The peak distance and their height provides information about the spin-orbit coupling strength, and their width directly points to violations of spin-charge separation. The ESR spectrum of a MWNT only exhibits a single narrow peak, whose location and linewidth provide information about the Rashba-type spin-orbit coupling and intrinsic electric fields.

We thank L. Forró for discussions. Support by the DFG under the Gerhard-Hess program and by the project PICT 99 3-6343 is acknowledged.

Z. Yao *et al.*, *ibid.* **402**, 273 (1999); H. Postma *et al.*, *Science* **293**, 76 (2001).

- [4] L. Forró and C. Schönberger, in: *Carbon nanotubes*, ed. by M.S. Dresselhaus *et al.*, Topics in Appl. Phys. **80** (Springer, 2001).
- [5] R. Egger and A.O. Gogolin, Phys. Rev. Lett. **79**, 5082 (1997); C.L. Kane, L. Balents, and M.P.A. Fisher, *ibid.* **79**, 5086 (1997).
- [6] L. Balents and R. Egger, Phys. Rev. Lett. **85**, 3464 (2000); Phys. Rev. B **64**, 035310 (2001).
- [7] A.V. Moroz, K.V. Samokhin and C.H.W. Barnes, Phys. Rev. Lett. **84**, 4164 (2000).
- [8] A. De Martino and R. Egger, Europhys. Lett. (in press), cond-mat/0109161.
- [9] We often put $\hbar = c = k_B = g_e \mu_B = 1$.
- [10] G.H. Chen and M.E. Raikh, Phys. Rev. B **60**, 4826 (1999).
- [11] N.E. Bonesteel, Phys. Rev. B **47**, 11 302 (1993).
- [12] A.O. Gogolin, A.A. Nersisyan, and A.M. Tsvelik, *Bosonization and Strongly Correlated Electron Systems* (Cambridge University Press, Cambridge, 1998).
- [13] S. Lemay *et al.*, Nature (London) **412**, 617 (2001).
- [14] L. Balents and M.P.A. Fisher, Phys. Rev. B **53**, 12 133 (1996).
- [15] Details will be published elsewhere.
- [16] For SWNTs, the orbital term can always be neglected.

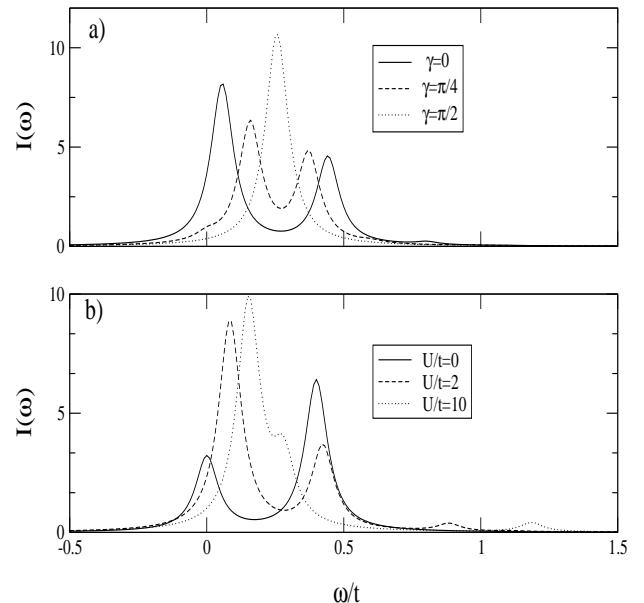


FIG. 1. Exact diagonalization results for the $T = 0$ ESR spectra of a Hubbard chain with $\lambda = 0.1$, $g_e \mu_B B/t = 0.2$, and artificial broadening $0.05t$. In (a) ESR spectra for $U/t = 1$ are shown for different angles γ between $\vec{\lambda}$ and \vec{B} . In (b) the U -dependence is shown for $\gamma = 0$. All results are for 12 lattice sites and 4 electrons.

- [1] M. Oshikawa and I. Affleck, Phys. Rev. Lett. **82**, 5136 (1999); cond-mat/0108424.
- [2] C. Dekker, Physics Today **52(5)**, 22 (1999). See also reviews on nanotubes in Physics World, No. 6 (2000).
- [3] M. Bockrath *et al.*, Nature (London) **397**, 598 (1999);